LBL-28672

Lawrence Berkeley Laboratory
UNIVERSITY OF CALIFORNIA

Physics Division

Presented at the XIV International Symposium on
Lepton and Photon Interactions, Stanford, CA,
August 6–12, 1989, and to be published in the Proceedings

Two-Photon Physics

R. Cahn

March 1990

TWO-WEEK LOAN COPY

This is a Library Circulating Copy which may be borrowed for two weeks.

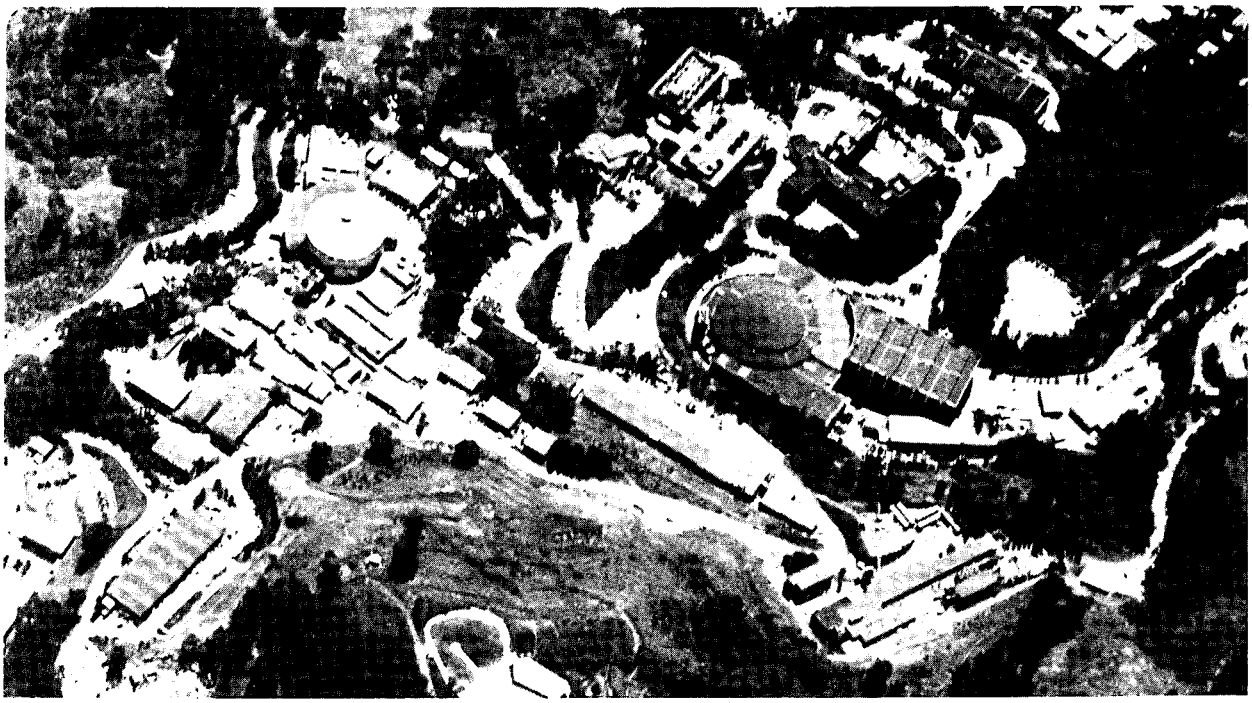

LBL-28672 Copy 2
Bldg. 50 Library.

Prepared for the U.S. Department of Energy under Contract Number DE-AC03-76SF00098.

DISCLAIMER

This document was prepared as an account of work sponsored by the United States Government. While this document is believed to contain correct information, neither the United States Government nor any agency thereof, nor the Regents of the University of California, nor any of their employees, makes any warranty, express or implied, or assumes any legal responsibility for the accuracy, completeness, or usefulness of any information, apparatus, product, or process disclosed, or represents that its use would not infringe privately owned rights. Reference herein to any specific commercial product, process, or service by its trade name, trademark, manufacturer, or otherwise, does not necessarily constitute or imply its endorsement, recommendation, or favoring by the United States Government or any agency thereof, or the Regents of the University of California. The views and opinions of authors expressed herein do not necessarily state or reflect those of the United States Government or any agency thereof or the Regents of the University of California.

March 2, 1990 LBL-28672

Two-Photon Physics *

To be included in the
Proceedings of the XIV International Symposium
on Lepton and Photon Interactions
Stanford, CA, August 6-12, 1989

Robert N. Cahn

Theoretical Physics Group
Physics Division
Lawrence Berkeley Laboratory
1 Cyclotron Road
Berkeley, California 94720

*This work was supported by the Director, Office of Energy Research, Office of High Energy and Nuclear Physics, Division of High Energy Physics of the U.S. Department of Energy under Contract DE-AC03-76SF00098.

Two-Photon Physics

Robert N. Cahn
Lawrence Berkeley Laboratory,
University of California,
Berkeley, CA 94720

ABSTRACT

Recent experimental results in two-photon physics are reviewed. Possibilities for future experimentation at high $\gamma\gamma$ collision energies are discussed.

1 Introduction

Two-photon physics has traditionally explored the low-energy regime of even-spin, even charge-conjugation states, although the range of two-photon physics has expanded in the last several years with the results on spin-one mesons. Despite its limited range, two-photon physics has commanded significant interest because the initial state is particularly simple and well understood. The major results have been in meson spectroscopy, studies of perturbative QCD, and low-energy hadronic phenomenology. This review covers results obtained since the 1987 Lepton-Photon Conference.

Will the future of two-photon physics be confined to the low-energy domain? Straightforward extensions like that available at LEP will not significantly increase the accessible domain. Only entirely new approaches can open up the high-energy domain. Some proposals to do so are discussed in the second part of the review.

Two-photon physics has been reviewed extensively. The report of Olsson [1] at the 1987 Lepton-Photon Conference gives comprehensive coverage up to that time. Two excellent sources are the reviews by Kolanoski and Zerwas [2] and by Cooper [3]. The proceedings of the 1988 Photon-Photon Workshop [4] are the source for many of the results obtained since the last Lepton-Photon meeting.

2 Pseudoscalar Mesons

Modern two-photon physics began with the observation of Francis Low [5] that the rate for the process $e^+e^- \to e^+e^-\pi^0$ was determined by the $\gamma\gamma$ width of the π^0. Measurements of the $\gamma\gamma$ widths of the π^0, η, and η', including some recent results, are shown in Table 2.1.

New results for the $\gamma\gamma$ widths have been reported for the η and η' by the ASP Collaboration at PEP using the $\gamma\gamma$ final state [6], and for the η' by the Mark II Collaboration in several decay modes [7]. The results of the Crystal Ball at DORIS II are particularly stunning for their excellent resolution, as seen in Fig. 2.1.

The $\gamma\gamma$ widths are determined by a matrix element of the electromagnetic current taken twice, between the pseudoscalar in question and the vacuum. The pure neutral states are

$$\begin{aligned} \pi^0 &= \frac{1}{\sqrt{2}}|u\bar{u} - d\bar{d}\rangle \\ \eta_8 &= \frac{1}{\sqrt{6}}|u\bar{u} + d\bar{d} - 2s\bar{s}\rangle \\ \eta_0 &= \frac{1}{\sqrt{3}}|u\bar{u} + d\bar{d} + s\bar{s}\rangle. \end{aligned} \tag{2.1}$$

The isoscalars can mix

$$\begin{aligned} |\eta\rangle &= \cos\theta|\eta_8\rangle - \sin\theta|\eta_0\rangle \\ |\eta\rangle' &= \sin\theta|\eta_8\rangle + \cos\theta|\eta_0\rangle, \end{aligned} \tag{2.2}$$

Collaboration	$\gamma\gamma$ width	Technique	Ref.
	π		
Crystal Ball	$7.7 \pm 0.5 \pm 0.5$ eV	$\gamma\gamma$	PR D38,1365(1988)
H. Atherton et al.	$7.25 \pm 0.18 \pm 0.11$ eV	lifetime	PL 158B,81,(1985)
G. Bellettini et al	11.8 ± 1.3 eV	Primakoff	NC 66A, 243, (1970)
A. Browman et al	8.0 ± 0.4 eV	Primakoff	PRL 37,1400(1974)
V. Kryshkin et al.	7.3 ± 0.6 eV	Primakoff	JETP 30, 1037 (1970)
	η		
Crystal Ball	$0.514 \pm 0.017 \pm 0.035$ keV	$\eta \to \gamma\gamma$	PR D38,1365 (1988)
ASP	$0.490 \pm 0.010 \pm 0.048$ keV	$\eta \to \gamma\gamma$	SLAC-PUB 4931
	η'		
JADE	$3.8 \pm 0.26 \pm 0.43$ keV	$\eta' \to \pi^+\pi^-\gamma$	PL 142B,125 (1984)
TPC/2γ	$4.5 \pm 0.3 \pm 0.7$ keV	$\eta' \to \pi^+\pi^-\gamma$	PR D35,2650(1987)
Mark II	$4.7 \pm 0.6 \pm 0.9$ keV	$\eta' \to \eta\pi^+\pi^-$	PRL 59, 2012 (1987)
Crystal Ball	$4.7 \pm 0.5 \pm 0.5$ keV	$\eta' \to \gamma\gamma$	PR D38, 1365 (1988)
JADE	$3.80 \pm 0.13 \pm 0.50$ keV	$\eta' \to \eta\pi^+\pi^-$	Shoresh p. 77.
CELLO	$4.7 \pm 0.2 \pm 1.0$ keV	$\eta' \to \pi^+\pi^-\gamma$	Shoresh p. 85.
ASP	$4.96 \pm 0.23 \pm 0.72$ keV	$\eta' \to \gamma\gamma$	SLAC-PUB 4931
Mark II	$4.61 \pm 0.32 \pm 0.60$ keV	$\eta' \to \rho\gamma$	LBL-26465(rev.)
Mark II	$4.37 \pm 0.62^{+0.98}_{-0.95}$ keV	$\eta' \to \eta\pi^+\pi^-$	LBL-26465(rev.)
Mark II	$4.60 \pm 0.49^{+0.68}_{-0.96}$ keV	$\eta' \to 4\pi$	LBL-26465(rev.)
TPC/2γ	$3.8 \pm 0.7 \pm 0.6$ keV	$\eta' \to \eta\pi^+\pi^-$	PR D38,1 (1988)

Table 2.1: Results on the $\gamma\gamma$ widths of the pseudoscalar mesons.

where we have assumed no other states (e.g., glueballs) are involved. The $\gamma\gamma$ widths of the physical states depend on the mixing angle and on the pseudoscalar decay constants F_π, F_0, and F_8. Perfect SU(3) symmetry requires $F_\pi = F_8$ while nonet symmetry would give, in addition, $F_0 = F_8$. The ratios of the $\gamma\gamma$ widths are given by [9]

$$\frac{\Gamma(\eta \to \gamma\gamma)}{\Gamma(\pi^0 \to \gamma\gamma)} = \left(\frac{m_\eta}{m_\pi}\right)^3 \left(\frac{1}{\sqrt{3}}\frac{F_\pi}{F_8}\cos\theta - 2\sqrt{\frac{2}{3}}\frac{F_\pi}{F_0}\sin\theta\right)^2 \quad (2.3)$$

$$\frac{\Gamma(\eta' \to \gamma\gamma)}{\Gamma(\pi^0 \to \gamma\gamma)} = \left(\frac{m_{\eta'}}{m_\pi}\right)^3 \left(\frac{1}{\sqrt{3}}\frac{F_\pi}{F_8}\sin\theta + 2\sqrt{\frac{2}{3}}\frac{F_\pi}{F_0}\cos\theta\right)^2 . \quad (2.4)$$

Chiral symmetry calculations indicate that $F_\pi/F_8 \approx 0.8$ [10,11]. If we use the measured $\gamma\gamma$ widths we can extract both the mixing angle and the ratio F_π/F_0. With values derived from Table 2.1

$$\begin{aligned} \Gamma(\pi^0 \to \gamma\gamma) &= 7.29 \text{ eV} \\ \Gamma(\eta \to \gamma\gamma) &= 0.51 \text{ keV} \\ \Gamma(\eta' \to \gamma\gamma) &= 4.4 \text{ keV} \end{aligned}$$

we find that if $F_\pi/F_8 = 1$, then $\theta = -17.5°$ and $F_\pi/F_0 = 0.945$. If instead we take $F_\pi/F_8 = 0.8$, then $\theta = -21.7°$ and $F_\pi/F_0 = 0.968$.

The $\gamma\gamma$ production of the η and η' has been studied as a function of the Q^2, the negative of the mass-squared, of one of the photons by the TPC/2γ Collaboration by single tagging. The data extend as far as $Q^2 = 4$ GeV^2, but most of the data are below $Q^2 = 2$ GeV^2. The data agree with expectations from the vector dominance model and also with a QCD-inspired result of Brodsky and Lepage [12], as

Collaboration	$\gamma\gamma$ width	Technique	Ref.
	$a_2(1320)$		
CELLO	$1.00 \pm 0.07 \pm 0.19$ keV	$\pi^+\pi^-\pi^0$	This conference
JADE	$0.84 \pm 0.07 \pm 0.15$ keV	$\pi^+\pi^-\pi^0$	Aachen $\gamma\gamma$ (1983)
JADE	$1.09 \pm 0.14 \pm 0.25$ keV	$\eta\pi^0$	Olsson/Shoresh
PLUTO	$1.06 \pm 0.18 \pm 0.19$ keV	$\pi^+\pi^-\pi^0$	PL 149B,427 (1984)
Crystal Ball (DORIS)	$1.14 \pm 0.20 \pm 0.26$ keV	$\eta\pi^0$	PR D33,1847 (1987)
TASSO	$0.90 \pm 0.27 \pm 0.16$ keV	$\pi^+\pi^-\pi^0$	ZfP C31,537 (1986)
TPC/2γ	$0.90 \pm 0.09 \pm 0.22$ keV	$\pi^+\pi^-\pi^0$	1987 EPS Meeting
Mark II	$1.03 \pm 0.13 \pm 0.22$ keV	$\pi^+\pi^-\pi^0$	LBL-26465
	$f_2(1270)$		
TPC/2γ	$3.2 \pm 0.1 \pm 0.4$ keV	$\pi^+\pi^-$	PRL 57, 404 (1986)
Crystal Ball	$3.26 \pm 0.16 \pm 0.28$ keV	$\pi^0\pi^0$	Marsiske/Shoresh
JADE	$3.09 \pm 0.10 \pm 0.38$ keV	$\pi^0\pi^0$	Olsson/Shoresh
CELLO	$3.0 \pm 0.1 \pm 0.5$ keV (prel.)	$\pi^+\pi^-$	Harjes/Shoresh
Mark II	$3.21 \pm 0.09 \pm 0.40$ keV	$\pi^+\pi^-$	Boyer/Shoresh
TOPAZ	$2.25 \pm 0.18 \pm 0.25$ keV (prel.)	$\pi^+\pi^-$	This conference
	$f_2'(1535)$		
TPC/2γ	$0.12 \pm 0.07 \pm 0.04$ keV	K^+K^-	PRL 57, 404 (1986)
ARGUS	0.054 ± 0.013 keV (prel.)	$f_2' \to K^+K^-$	Nilsson/Shoresh
PLUTO	$0.10^{+0.04}_{-0.03}{}^{+0.03}_{-0.02}$ keV	$f_2' \to K_S^0K_S^0$	Feindt/Shoresh
CELLO	$0.11^{+0.03}_{-0.02} \pm 0.02$ keV	$f_2' \to K_S^0K_S^0$	Feindt/Shoresh
	$\pi_2(1680)$		
Crystal Ball	1.4 ± 0.3 keV	$\pi^0\pi^0\pi^0$	Muryn/Shoresh
CELLO	$1.3 \pm 0.3 \pm 0.2$ keV	$\pi^+\pi^-\pi^0$	This conference

Table 3.1: Recent measurements of $\gamma\gamma$ widths of tensor mesons.

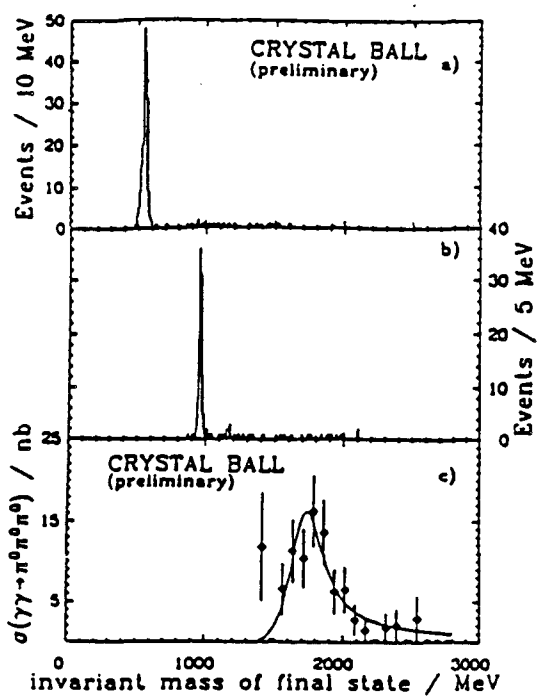

Figure 2.1: Results of the Crystal Ball Collaboration in the 6 γ final state. The top figure shows $\eta \to 3\pi^0 \to 6\gamma$. The middle figure show $\eta' \to \eta\pi^0\pi^0 \to 6\gamma$. The bottom figure shows $\pi_2(1680) \to 3\pi^0 \to 6\gamma$. Ref. [8]

seen in Fig. 2.2.

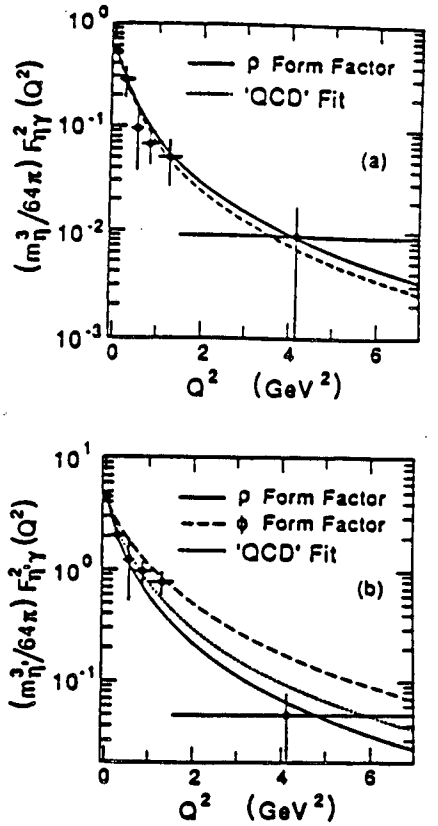

Figure 2.2: Results from the TPC/2γ Collaboration for the form factor squared as a function of Q^2 in the couplings $\eta\gamma\gamma^*$ and $\eta'\gamma\gamma^*$ [13].

3 Tensor Mesons

Numerous measurements of the $\gamma\gamma$ widths of tensor mesons have been made since the last Lepton-Photon Conference, many but not all of which were reported at the Shoresh meeting. A summary appears in Table 3.1. Crystal Ball [14], JADE [15], CELLO [16], and Mark II [17] all reported on the $f_2(1270)$ at Shoresh, with widths near 3.1 keV. A preliminary result from TOPAZ [18] at TRISTAN is substantially lower. The measurements in the $\pi^+\pi^-$ channel are plagued with backgrounds from $e^+e^- \to e^+e^-\mu^+\mu^-$ and $e^+e^- \to e^+e^-e^+e^-$. It is reassuring that the bulk of the measurements in the charged $\pi^+\pi^-$ channel agree with those in the neutral $\pi^0\pi^0$ channel. (It must be borne in mind however, that assigning all the observed events in the appropriate mass range to the f_2 may not be correct as discussed further in Sections 5 and 6 below [17].) The results of the Crystal Ball Collaboration on the all-photon final states are especially impressive, as shown in Fig. 3.1.

The isovector $a_2(1320)$ has been seen in $\gamma\gamma$ collisions in both its 3π and $\eta\pi^0$ decay channels. The data from the Crystal Ball are shown in Fig. 3.1.

If the 2^{++} tensors are described as nonrelativistic quark-antiquark bound states, their production in $\gamma\gamma$ collisions should produce only the helicity ± 2 states and no helicity-0 states. Generally this is assumed in extrapolating the observed decays to the full angular region. Angular distributions from JADE [15] on $f_2 \to \pi^0\pi^0$, from PLUTO [19] on $f_2'(1535) \to K_S^0 K_S^0$, and from the Crystal Ball [20] on $a_2(1320)$ support this assumption.

The 2^{++} tensor meson mixing is nearly ideal, so

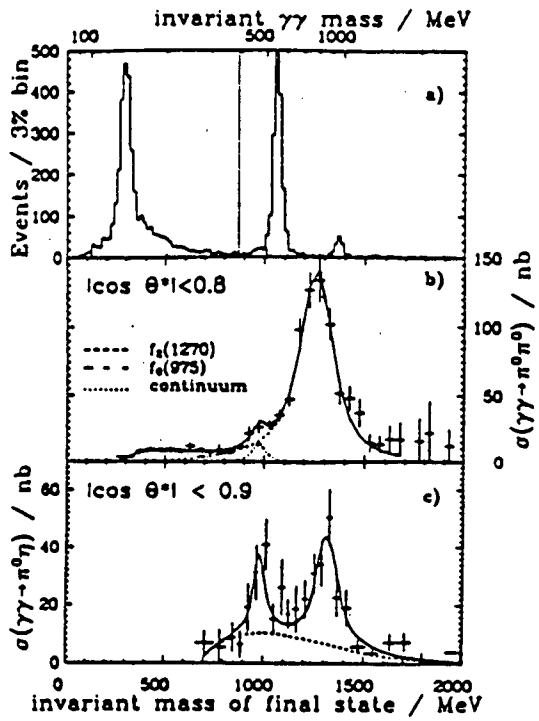

Figure 3.1: Results of the Crystal Ball Collaboration in the 4 γ final state. In a) and b) data for $\gamma\gamma \to \pi^0\pi^0 \to 4\gamma$ are displayed. In c) data for $\gamma\gamma \to \pi^0\eta \to 4\gamma$ are displayed (Ref. [8]). In a) and b) the $f_2(1270)$ is apparent together with a small signal for the $f_0(975)$. In c) the $a_0(980)$ and the $a_2(1320)$ are readily seen.

it is appropriate to describe the physical states as

$$\begin{aligned} f &= \cos\lambda \frac{1}{\sqrt{2}}|u\bar{u} + d\bar{d}\rangle + \sin\lambda|s\bar{s}\rangle \\ f' &= -\sin\lambda \frac{1}{\sqrt{2}}|u\bar{u} + d\bar{d}\rangle + \cos\lambda|s\bar{s}\rangle \\ a_2 &= \frac{1}{\sqrt{2}}|u\bar{u} - d\bar{d}\rangle. \end{aligned} \tag{3.1}$$

Ignoring the mass differences and assuming that there is no breaking of the full symmetry (U(3)) of the quarks, we obtain the relations

$$\Gamma(f_2 \to \gamma\gamma)/\Gamma(a_2 \to \gamma\gamma) = 3\sin^2(\lambda + \beta)$$

$$\Gamma(f_2' \to \gamma\gamma)/\Gamma(a_2 \to \gamma\gamma) = 3\cos^2(\lambda + \beta) \tag{3.2}$$

$$3\Gamma(a_2 \to \gamma\gamma) = \Gamma(f_2 \to \gamma\gamma) + \Gamma(f_2' \to \gamma\gamma), \tag{3.3}$$

where

$$\tan\beta = 5/\sqrt{2}. \tag{3.4}$$

From Table 3.1 we obtain the nominal values

$$\begin{aligned} \Gamma(a_2 \to \gamma\gamma) &= 1.0 \text{ keV} \\ \Gamma(f_2 \to \gamma\gamma) &= 3.2 \text{ keV} \\ \Gamma(f_2' \to \gamma\gamma) &= 0.10 \text{ keV}, \end{aligned}$$

which yield $\lambda = 6°$ and are in rather good agreement with Eq. 3.3.

The 2^{-+} axial tensors can be made from a d-wave $q\bar{q}$ state. The $\pi_2(1670)$ (formerly the A_3) decays into $f_2\pi$ and $\rho\pi$ with a width of 250 MeV. It has been observed by the Crystal Ball [21] in $3\pi^0$ (see Fig. 2.1) and by CELLO [22] in $\pi^+\pi^-\pi^0$. The $\gamma\gamma$ width is more than 1 keV, larger than that of the a_2. This is perhaps surprising since in a nonrelativistic quark model the d-wave decay involves the second derivative of the wave function at the origin, rather than just the first derivative, which enters for p-wave states like the a_2.

4 η_c

Measuring the $\gamma\gamma$ width of the η_c has been a prominent challenge because there is a clear prediction for the value based on a nonrelativistic $c\bar{c}$ model:

$$\Gamma(^1S_0 \to \gamma\gamma) = \frac{12\alpha^2}{M^2}\left(\frac{2}{3}\right)^4 |R(0)|^2. \tag{4.1}$$

This can be compared to the prediction for the width of $\psi \to e^+e^-$:

$$\Gamma(^3S_1 \to e^+e^-) = \frac{4\alpha^2}{M^2}\left(\frac{2}{3}\right)^2 |R(0)|^2 = 4.7 \text{ keV}. \tag{4.2}$$

where the value given is the experimental one. A calculation [23] of the effect of the hyperfine interaction, responsible for the η_c - ψ splitting, increases the prediction for the $\gamma\gamma$ width by about 25%, to a little less than 8 keV.

The new TASSO result [24] is larger than the predicted value, but not inconsistent with it (See Table 4.1). The TPC/2γ Collaboration is unique in measuring the $4K$ final state [25]. Its results are similar to those of the Mark II Collaboration [26]. The CLEO Collaboration has reported [27] on both the

$K_S K\pi$ and $K^{*0}K\pi$ channels, again finding general agreement with the predicted value.

While the results from $\gamma\gamma$ collisions and from the complementary $p\bar{p}$ experiment, R704, at CERN [28] are consistent with the theoretical prediction, the uncertainties remain disappointingly large. This is clearly one measurement that could benefit from greatly increased statistics.

5 Scalar Mesons

Of the extensively investigated multiplets, the scalar is the most enigmatic. The study of the $\gamma\gamma$ widths of the scalars can provide important insights into the problems raised by the nonstrange 0^{++} mesons, as discussed by Chanowitz at the 1988 Two-Photon Conference [29]. In the nonrelativistic quark model, the $\gamma\gamma$ widths of the scalars and tensors are simply related since both are ^{3}P states:

$$\frac{\Gamma(0^{++} \to \gamma\gamma)}{\Gamma(2^{++} \to \gamma\gamma)} = \frac{15}{4} \times \text{phase space.} \tag{5.1}$$

However, a glance at Tables 3.1 and 5.1 reveals

$$\frac{\Gamma(a_0(975))}{\Gamma(a_2(1320))} \approx 0.2 - 0.3 \tag{5.2}$$

$$\frac{\Gamma(f_0(980))}{\Gamma(f_2(1270))} \approx 0.1 \tag{5.3}$$

in gross violation of Eq. (5.1), even if phase space effects are included.

Not only are the widths of the scalars much too small, their masses seem to be as well. The strange member of the multiplet is apparently the $K^*(1430)$. Indeed there is a candidate scalar, $f_0(1400)$, in the correct mass range. This leaves two problems [29]: where are the higher mass scalars with their few keV $\gamma\gamma$ widths and what are the $f_0(975)$ and the $a_0(980)$? It has been suggested that the two light scalars are actually $qq\bar{q}\bar{q}$ states [30] or $K\bar{K}$ molecules[31]. As for the yet-to-be-observed more massive scalars, there is the provocative suggestion that they are lying underneath the tensors [29]. To determine whether this is so requires a careful partial-wave analysis.

6 $\pi\pi$ Final State

The $\pi\pi$ final state is of interest not only because of the problems in the scalar channel near 1 GeV, but also because of its special simplicity in the low-energy range. There the constraints of analyticity and unitarity provide a useful handle on the amplitude [32]. At the same time, it is an excellent subject for an analysis based on chiral symmetry [33,34].

Morgan and Pennington [35] have emphasized the importance of a proper treatment of the $\gamma\gamma \to \pi\pi$ data that incorporates the effects of unitary and is consistent with what is known about $\pi\pi$ scattering. Preliminary results from such analysis using Mark II and Crystal Ball data [14] are shown in Fig. 6.1. There is a suggestion here of some scalar resonance hiding under the f_2 as hypothesized by Chanowitz, though a complete analysis remains to be done.

7 Glueballs

Glueballs are gluonic bound states that should couple feebly to $\gamma\gamma$, while coupling strongly to *gluon-gluon*. Limits on the $\gamma\gamma$ widths of glueball candidates are given in Table 7.1. Chanowitz [36] has proposed a quantitative measure, stickiness, S, that should help identify glueballs:

$$S_X = \frac{\Gamma(\psi \to \gamma X)}{\Gamma(X \to \gamma\gamma)} \cdot \frac{LIPS(X \to \gamma)}{LIPS(\psi \to \gamma X)}, \tag{7.1}$$

where $LIPS$ is the Lorentz-invariant phase space factor. The status of the glueball candidates $\eta(1430)$, $f_2(1720)$, and $X(2230)$ has been reviewed by Feindt [37]. The pertinent data are from TPC/2γ [38], PLUTO [39,40], CELLO [41,42], and Mark II [43].

From these numbers and the ψ radiative decays, Feindt derives the stickiness ratios [37]:

Collaboration	$\gamma\gamma$ width	Technique	Ref.
		$\eta_c(2980)$	
PLUTO	28 ± 15 keV	$K_S K\pi$	PL 167B,120(1986)
TASSO	$19.9 \pm 6.1 \pm 8.6$ keV	$K_S K\pi, K^+K^-\pi^+\pi^-, 4\pi$	ZfP C41,533(1989)
TPC/2γ	$6.4^{+5.0}_{-3.4}$ keV	$4K$	PRL 60,2533(1988)
Mark II	8 ± 6 keV	$K_S K\pi$	Gidal, Berkeley 1986
CLEO	$9.4^{+3.7}_{-3.0} \pm 2.7$ keV	$K_S K\pi$	Cornell June 1989
CLEO	$8.5^{+4.6}_{-4.2} \pm 3.9$ keV	$K^* K\pi$	Cornell June 1989
R704	$4.3^{+3.4}_{-3.7} \pm 2.4$ keV	$p\bar{p}$ annihilation	PL 187B,191(1987)

Table 4.1: Results for the $\gamma\gamma$ width of the η_c.

Collaboration	$\Gamma(\rightarrow \gamma\gamma)B(a_0 \rightarrow \eta\pi)$	Technique	Ref.
		$a_0(980)$ (δ)	
JADE	$0.29 \pm 0.05 \pm 0.14$ keV	$\eta\pi^0$	Olsson/Shoresh
Crystal Ball	$0.19 \pm 0.07^{+0.10}_{-0.07}$ keV	$\eta\pi^0$	PR D36,2633 (1987)
		$f_0(975)$ (S^*)	
Mark II	$0.24 \pm 0.06 \pm 0.15$ keV	$\pi^+\pi^-$	Boyer/Shoresh
Crystal Ball	$0.31 \pm 0.14 \pm 0.11$ keV	$\pi^0\pi^0$	Marsiske/Shoresh

Table 5.1: Measurements of $\gamma\gamma$ widths of scalar mesons.

$$S_{\pi^0} : S_\eta : S_{\eta'} : S_\iota = 0.02 : 1 : 4 : 80(95\%C.L.) \tag{7.2}$$

and

$$\begin{aligned} &S_{f_2} : S_{f_2'} : S_{f_2(1720)} : S_{X(2230)}; \\ &= 1 : 13 :> 28(95\%C.L.) :> 9(95\%C.L.). \end{aligned} \tag{7.3}$$

The large apparent stickiness of the f_2' is just a reflection of its small $\gamma\gamma$ width caused by the small charge of its quarks. The large stickiness of the $\iota = \eta(1430)$ is not only impressive, it understates the case! Combining the data from the various experiments for the limit on $\Gamma(\eta(1430) \rightarrow \gamma\gamma)B(K\overline{K}\pi)$, Feindt [37] derives an upper limit of 0.75 keV and a corresponding stickiness greater than 128.

An alternative explanation for nonexotic "extra" states is that they are radial excitations. Radial excitations should have $\gamma\gamma$ widths that are smaller, but not very much smaller, than ordinary mesons. The possibility that the radially excited pseudoscalar multiplet consists of $\pi(1300), \kappa(1460), \eta(1280)$, and $\eta(1390)$ has been examined by Chanowitz [29]. A primary difficulty is the Crystal Ball limit

$$\Gamma(\eta(1280, 1390) \rightarrow \gamma\gamma)B(\eta\pi\pi) < 0.3 \text{ keV} \tag{7.4}$$

at 90% C.L., which applies to states below 1500 MeV with widths less than 50 MeV. The anticipated $\gamma\gamma$ widths for radially-excited states would be significantly greater [29].

8 Spin-One Mesons

The discovery in 1986 by the TPC/2γ Collaboration of a spin-1 meson produced in $\gamma^*\gamma$ collisions demonstrated the versatility of two-photon experimentation. There are now results from several col-

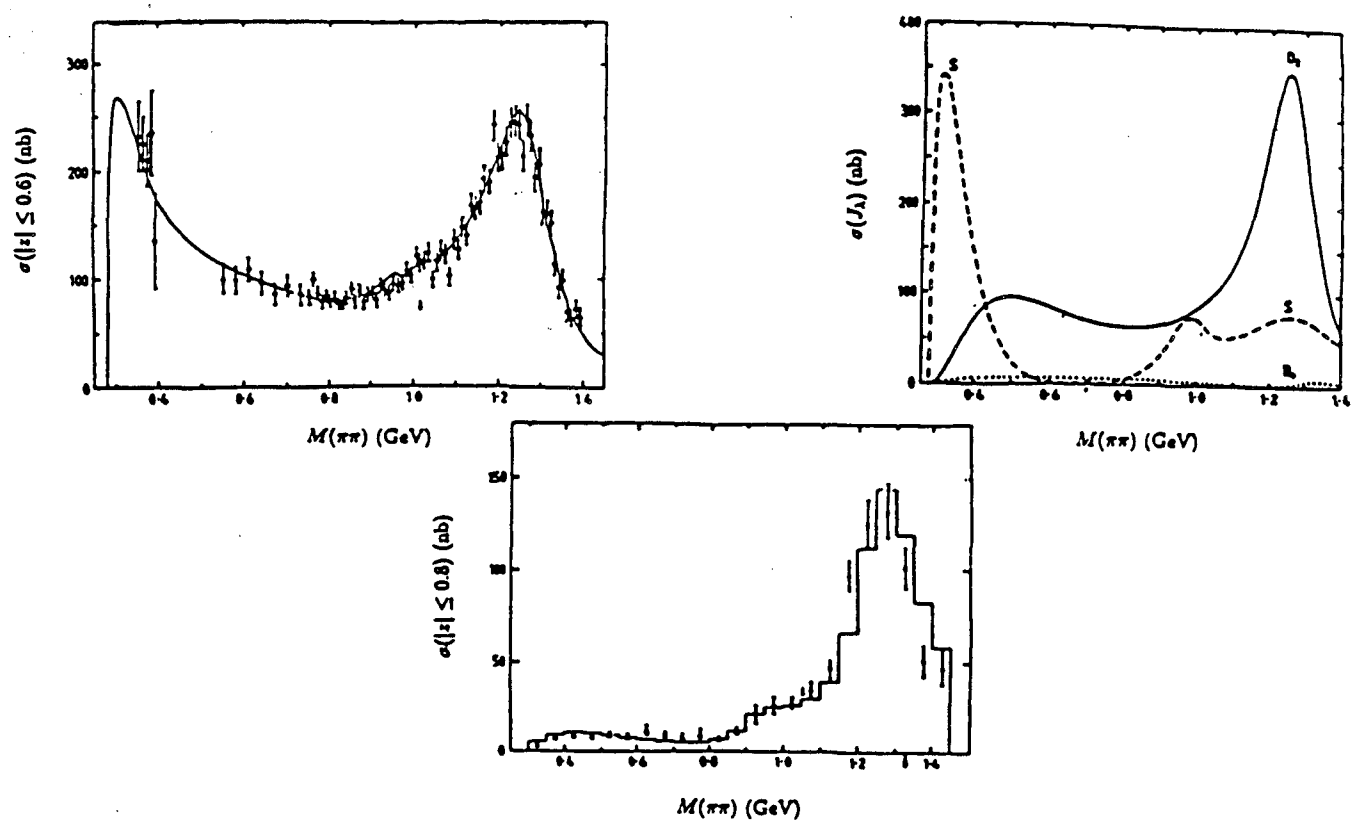

Figure 6.1: Preliminary results of fits by D. Morgan and M. Pennington to Mark II data [17] on $\gamma\gamma \to \pi^+\pi^-$ and Crystal Ball data [14] on $\gamma\gamma \to \pi^0\pi^0$. The figure on the left shows the $\pi^+\pi^-$ data. The middle figure shows the $\pi^0\pi^0$ data. The figure on the right shows the various partial wave contributions to $\pi\pi$ scattering. Beneath the D_2 (f_2, helicity 2) is a contribution from S (f_0).

laborations, summarized in Table 8.1, on both the $f_1(1425)$ and the previously known $f_1(1285)$ (the old D(1285)).

The pioneering theoretical investigation was done by Renard [44]. While Yang's Theorem forbids a spin-1 particle from decaying into two real photons, decays into a real photon and a virtual one are allowed. Of course the coupling vanishes as the virtual photon becomes real. Thus the experimental signature for a spin-1 meson in $\gamma\gamma$ collisions is the appearance of a resonance when one electron is tagged, and so one photon is measured to be quite virtual. The resonance is essentially absent in the untagged data (or better, antitagged data).

Because the $\gamma^*\gamma$ width vanishes as the virtual photon becomes real, it is necessary to adopt a new measure of the coupling. The conventional one is

$$\tilde{\Gamma} = \lim_{Q^2 \to 0} \frac{M^2}{Q^2} \Gamma(Q^2) \tag{8.1}$$

where M is the mass of the resonance. Unfortunately, there is another convention to establish, that for $\Gamma(Q^2)$. For the same data Mark II and CELLO would report values twice as large as TPC/2γ and JADE. The Mark II - CELLO convention seems preferable [45], and we use it throughout.

For lack of a good alternative, the $\gamma^*\gamma$ width of the f_1 states can be estimated using a nonrelativistic quark model. The same model gives a prediction for the $\gamma\gamma$ widths of the $J = 0$ and $J = 2$ states in the same term, ^3P. If the $q\bar{q}$ wave function is written as $R(r)$ times an angular and spin wave function, with $\int dr\, r^2 R^2(r) = 1$, then all the widths are pro-

Collaboration	$\Gamma B(\rightarrow KK\pi)$	Technique	Ref.
		$\eta(1430)$	
TPC/2γ	1.6 keV	$K_SK\pi$	PRL 57, 51 (1986)
Mark II	1.5 keV	$K_SK\pi$	PRL 59, 2016 (1987)
CELLO	1.2 keV	$K_SK\pi$	ZfP 42, 367 (1989)
PLUTO	2.7 keV	$K_SK\pi$	Feindt Thesis
		$f_2(1720)$	
PLUTO	0.07 keV	K_SK_S	ZfP 37, 329 (1988)
CELLO	0.11 keV	K_SK_S	ZfP 43, 91 (1988)
		$X(2230)$	
PLUTO	0.07 keV	K_SK_S	ZfP 37, 329 (1988)
CELLO	0.12 keV	K_SK_S	ZfP 43, 91 (1988)

Table 7.1: Limits on the $\gamma\gamma$ widths of glueball candidates. See references for details of assumptions made in determining the upper limits on the $\gamma\gamma$ widths. For the $\eta(1430)$, the Mark II number is obtained by assuming $\Gamma(\eta(1430)) = 60$ MeV.

portional to $[R'(0)]^2$. In particular,

$$\Gamma(f_2 \rightarrow \gamma\gamma) = \frac{576}{5}\alpha^2\langle e_q^2\rangle^2\frac{|R'(0)|^2}{M^4} \qquad (8.2)$$

$$\Gamma(f_1 \rightarrow \gamma\gamma^*) = 192\alpha^2\langle e_q^2\rangle^2\frac{|R'(0)|^2}{M^4}\frac{Q^2}{M^2}. \qquad (8.3)$$

If we use $\Gamma(f_2 \rightarrow \gamma\gamma) = 3.2$ keV, we predict for an f_1 with the same quark content $\bar{\Gamma} = (5/3) \times 3.2$ keV $= 5.3$ keV. The factor for the quark charges is 1/81 for a pure $s\bar{s}$ state, 25/162 for a pure isoscalar $(u\bar{u} + d\bar{d})/\sqrt{2}$ state, and 1/18 for the isovector $(u\bar{u} - d\bar{d})/\sqrt{2}$. Thus if the state observed at 1425 MeV were the old E that decays predominantly to strange states, the $\gamma^*\gamma$ width would be expected to be much smaller than that of the entirely nonstrange $f_1(1285)$.

Perhaps then the state at 1425 MeV is not the old E. Chanowitz has proposed that it might not even have $J^{PC} = 1^{++}$, but be an exotic 1^{-+} instead [46]. He shows that if the state is a meikton $(u\bar{u} + d\bar{d})g/\sqrt{2}$ it would have a large coupling to $\gamma\gamma$ while still producing the KK^* final state. The 1^{++} and 1^{-+} alternatives can be distinguished by measuring the distribution of the angle between the normal to the decay plane containing the $K\overline{K}\pi$ and the beam direction. If the production is entirely through one transverse and one longitudinal photon, the angular distributions are unique: $1 + \cos^2\theta$ for 1^{++} and $1 - \cos^2\theta$ for 1^{-+} [47]. Unfortunately, there are contributions from pairs of transverse photons as well, though these are suppressed at low Q^2. Within the nonrelativistic quark model there is a definite connection between the longitudinal–transverse and transverse–transverse production. However, for the exotic state that cannot be a $q\bar{q}$ there is no simple model. Thus to exclude reliably the exotic interpretation, only data at Q^2 small should be used. Data from JADE, CELLO, Mark II, and TPC/2γ prefer the 1^{++} assignment to 1^{-+}, but cannot provide a definitive answer [48]. The data for the $f_1(1285)$ quite convincingly choose $J^P = 1^+$ [48].

The CELLO Collaboration has done an extensive investigation of the $f_1(1425)$ within the limitations imposed by the data sample of 17 candidate events. They find that the final state is dominantly KK^* and use this to provide additional tests of the parity through angular distributions. Their results for the squares of the transverse-transverse and transverse-longitudinal form factors are shown in Fig.8.1. The total cross section constrains the results to lie in a band for each of four Q^2 intervals. The angular dis-

Collaboration	$\overline{\Gamma}B(\rightarrow KK\pi)$	Technique	Ref.
	$f_1(1425)$		
TPC/2γ	$2.6 \pm 1.0 \pm 0.6$ keV	ρ form factor	PR D38,1 (1988)
TPC/2γ	$1.26 \pm 0.48 \pm 0.3$ keV	ϕ form factor	PR D38,1 (1988)
Mark II	$3.2 \pm 1.4 \pm 0.6$ keV	ρ form factor	PRL 59,2016(1987)
Mark II	$2.1 \pm 1.0 \pm 0.4$ keV	ϕ form factor	PRL 59,2016(1987)
JADE	$4.6^{+2.0}_{-1.8} \pm 1.6$ keV	ρ form factor	ZfP C42,355(1989)
JADE	$3.0^{+1.2}_{-1.0} \pm 1.0$ keV	ϕ form factor	ZfP C42,355(1989)
CELLO	$3.0 \pm 0.9 \pm 0.7$ keV	ρ form factor	ZfP C42,367(1989)
CELLO	$1.4 \pm 0.4 \pm 0.3$ keV	ϕ form factor	ZfP C42,367(1989)
	$f_1(1285)$ (D)		
TPC/2γ	$4.8 \pm 1.0 \pm 1.0$ keV	$\eta\pi\pi$	PR D38,1 (1988)
Mark II	$9.4 \pm 2.5 \pm 1.7$ keV	$\eta\pi\pi$	PRL 59,2016(1987)
JADE	$3.6 \pm 0.6 \pm 0.8$ keV	$\eta\pi\pi$	Olsson/Shoresh
CELLO	$7.2 \pm 2.2 \pm 2.4$ keV	$\eta\pi\pi$	Ahme/Shoresh

Table 8.1: Measurements of $\gamma\gamma$ widths of spin-one mesons. The Mark II - CELLO convention is used.

tributions reflect the ratio of transverse-transverse to transverse-longitudinal. As $Q^2 \rightarrow 0$, the latter must dominate the former by a power of Q^2. For the 1^{++} hypothesis, the transverse-longitudinal component is found to dominate and, except in the highest Q^2 bin, no transverse-transverse component is required and only a 95% C.L. can be plotted. In contrast, for the 1^{-+} hypothesis, the transverse-transverse piece predominates, even at the lowest Q^2 where no transverse-longitudinal component is found in the fit. Thus the exotic spin-parity assignment might solve the puzzle of why the $f_1(1425)$ has too large a $\gamma\gamma$ width to be an $s\bar{s}$ state, but it raises the dynamical puzzle of the dominance of transverse-transverse production at low Q^2.

9 Vector-Vector Final States

The vector dominance model suggests that the vector-vector final state in $\gamma\gamma$ interactions ought to be especially interesting. The ARGUS Collaboration has made extensive contributions to the data on these channels. While there are a variety of theoretical models, none is successful in dealing with the entire data sample.

Some of the recent experimental results are summarized in Table 9.1, which shows that roughly speaking there are three distinct categories: those with a large cross section ($\rho^0\rho^0$, $K^{*+}\overline{K}^{*-}$), those with a medium cross section ($\rho^+\rho^-$, $\rho\omega$, $\omega\omega$), and those with a small cross section ($K^{*0}\overline{K}^{*0}$, $\phi\phi$, $\rho\phi$, $\omega\phi$). The energy at which the peak cross section occurs also varies from one final state to another. The striking difference between the charged and neutral $\rho\rho$ channels precludes a simple s-channel resonance explanation.

Among the theoretical models are the t-channel Factorization Model (TCFM) [52], $qq\overline{q}\overline{q}$ models [53,54], and a QCD-motivated model [55]. The first seeks to identify specific t-channel exchanges and extract them from photoproduction data according to

$$\sigma(\gamma\gamma \rightarrow V_1V_2) = \sum_i \frac{\sigma^i(\gamma p \rightarrow V_1 p)\sigma^i(\gamma p \rightarrow V_2 p)}{\sigma^i(pp \rightarrow pp)} \frac{F^2_{\gamma p}}{F_{pp}F_{\gamma\gamma}}, \tag{9.1}$$

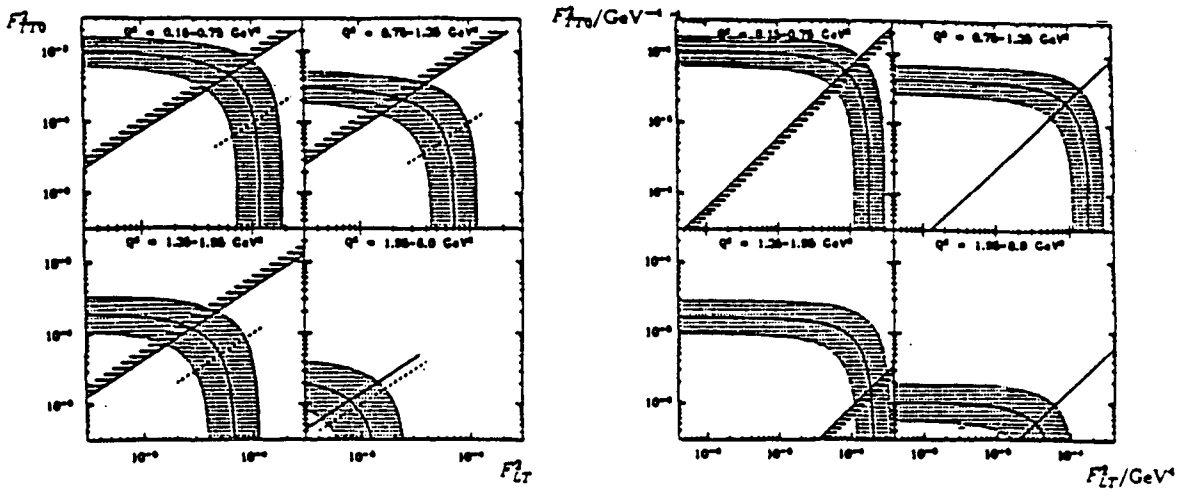

Figure 8.1: Analysis from the CELLO Collaboration for the squares of the form factors F_{TT}^2 and F_{TL}^2 for the $\gamma^*\gamma$ couplings to the $f_1(1425)$. The left set assumes the state has $J^{PC} = 1^{++}$; the right assumes 1^{-+}. The bands show allowed (1σ) regions. The angular distribution analysis prefers results along the diagonal lines in three of the figures. For the remaining five the horizontal lines indicate regions excluded at 95% C. L. The figures show that the 1^{++} assignment requires dominance by the transverse-longitudinal production while the 1^{-+} requires dominance by the transverse-transverse production, even at low Q^2, in contradiction with expectations.

where the F_{ij}s are flux factors. The second relies on the predictions for $qq\overline{q}\overline{q}$ states [30]. Interference between nearly degenerate $qq\overline{q}\overline{q}$ states can account for some of the intricate behavior in the data. The third considers three perturbative diagrams for $\gamma\gamma \to (q\overline{q})(q'\overline{q})$ that include one exchange of a gluon. The successes and failures of these models have been reviewed previously [2,56,57].

The TCFM does well for the $\rho^0\rho^0$ data, acceptably for $\rho\omega$, and poorly for $\omega\omega$ [57], while pleading ignorance in the instance of $K^*\overline{K}^*$. The $qq\overline{q}\overline{q}$ model has trouble with the $K^*\overline{K}^*$ states. Achasov and Shestakov [58] proposed a K-exchange model to explain the $K^{*0}\overline{K}^{*0}$ data, but it predicts that the cross section for the charged $K^*\overline{K}^*$ final state will be smaller than that for the neutral, which contradicts the data. Li and Liu find that permitting mixing among the $qq\overline{q}\overline{q}$ states enables them to fit the data [59]. The QCD motivated model also is undone by the $K^*\overline{K}^*$ data since it underestimates the absolute cross sections by about a factor of 8. It seems that understanding hadronic dynamics at low energy is difficult indeed, even when the initial state is as simple as $\gamma\gamma$.

One instance of inclusive vector production is notable: D^*. Production of charm in photon-photon collisions, like that of u quarks, is enhanced by a factor of 16 relative to that of d and s. Of course, the threshold is rather high for $\gamma\gamma$ collisions, but evidence has been presented previously for charm production by the JADE Collaboration [49] and the TPC/2γ Collaboration [50]. Now the TASSO Collaboration has reported the observation of inclusive $D^{*\pm}$ production and $D^0\overline{D}^0$ production [51]. The detection of D^* is facilitated by the small mass difference between the D and D^*. Models must be used to compare the observed cross sections to the predictions of the quark model. The TASSO observations indicate a cross section larger than expected, a result that agrees with the JADE results but not those of the TPC/2γ Collaboration.

10 Baryons

New data from ARGUS [60] and the TPC/2γ Collaboration [61] have become available for exclusive states containing baryons. The ARGUS data cover the final states $p\overline{p}$, $p\overline{p}\pi^0$, $p\overline{p}\pi^+\pi^-$, and $p\overline{p}\pi^+\pi^-\pi^0$.

Process	Collaboration	Ref.	Features
$\rho^0\rho^0$	PLUTO	ZfP C38,521 (1988)	100 nb @ 1.5 GeV
	TPC/2γ	PR D37, 28 (1988)	120 nb @ 1.3 GeV
$\omega\omega$	ARGUS	PL 198B,577 (1987)	16 nb @ 1.9 GeV
$\phi\phi$	ARGUS	PL 210B,273 (1988)	< few nb
	TPC/2γ	PR D37,28 (1988)	< few nb
$\rho\omega$	ARGUS	PL 196B,101 (1987)	30 nb @ 1.9 GeV
	TPC/2γ	Ronen/Shoresh	36 nb @ 1.8 GeV
$\rho\phi$	TPC/2γ	PR D37,28 (1988)	< few nb
	ARGUS	PL 198B,255 (1988)	< 1.0 nb
$\omega\phi$	ARGUS	PL 210B,273 (1988)	< few nb
$\rho^+\rho^-$	CELLO	PL 218B,493 (1989)	22 nb @ 1.9 GeV
	ARGUS	PL 217B,205 (1989)	30 nb @ 1.6 GeV
$K^{*+}K^{*-}$	ARGUS	PL 212B,528 (1988)	50 nb @ 1.4 GeV
$K^{*0}\overline{K}^{*0}$	ARGUS	PL 198B,255 (1988)	7 nb @ 2 GeV

Table 9.1: Results for the $\gamma\gamma$ production of vector-vector final states.

The TPC 2γ data are for $p\bar{p}\pi^+\pi^-$. Neither group finds an established signal for $\Delta^0\overline{\Delta}^0$, and both find only small signals for $\Delta^{++}\overline{\Delta}^{--}$ compared with the $p\bar{p}$ signal.

This result is contrary to the very naive expectation that the Δ^{++}, having twice the charge of the proton (which is in the same SU(6) multiplet), should be produced 16 times as frequently. It is even further from early predictions of models based on perturbative QCD that the ratio should be 50 [62]. However, a newer model using QCD sum-rule wavefunctions [63], finds a ratio between 0.5 and 2.

11 Structure Functions and Total Cross Section

The most elegant goal of two-photon physics has been to investigate the structure of the photon itself by scattering a virtual photon from a nearly real one. This has attracted enormous theoretical attention since the demonstration by Witten that the structure function of the photon in the high Q^2 limit is completely calculable in QCD [64]. Unfortunately, at subasymptotic energies there are important contributions from nonperturbative hadronic interactions. While these can be modeled, there is inevitably a problem of double counting interactions. Moreover, the perturbative calculation develops a singularity at $x = 0$, where $x = Q^2/2M\nu$ represents the fraction of the target photon's momentum carried by the struck quark. That singularity is of course canceled by one in the nonpertubative calculation, so that the sum, which is physical, is free of singularities.

A controversy continues over whether it is then possible to extract effectively the scale parameter, Λ_{QCD}, from the data available. An optimistic view is taken by Berger and Wagner [65] in their extensive review of two-photon physics. From the data available to them, they concluded

$$\Lambda_{\overline{MS}} = 195^{+60}_{-40} \text{ MeV}. \tag{11.1}$$

A pessimistic view is taken by Field, Kapusta, and Poggioli [66]. They nicely organize the calculation of the structure function so that the cancellation of the singularity is manifest. Their perturbative calculation is cutoff at some particular value of the

transverse momentum of the struck quark. For lower values of the transverse momentum the photon is regarded as a hadronic object with its own structure function. The resulting expression is less sensitive to the value of Λ_{QCD} than the originally derived expression of Witten and thus less effective for the purpose of deducing Λ_{QCD} from the data.

Frazer has provided a convenient analysis [67] of this situation using expressions [68] in the variable x rather than the more opaque ones for the moments. His conclusion is that there is some truth in both the pessimistic and optimistic positions: The sensitivity to Λ_{QCD} is indeed reduced, but at large values of Q^2 and x, say $Q^2 = 100$ GeV^2 and $x = 0.9$, the reduction is not great.

Photon structure function results were submitted to this conference by the TPC/2γ Collaboration [69] and by the AMY Collaboration [70]. The TPC/2γ data are presented for

$$\sigma_{\gamma\gamma}(W, Q^2) = \frac{4\pi^2\alpha}{Q^2} F_2^\gamma(x, Q^2), \qquad (11.2)$$

with $x = Q^2/(Q^2 + W^2)$. The data are compared to the vector dominance model (VDM) and the quark parton model (QPM). The VDM contribution has a Q^2 variation $(1 + Q^2/m_V^2)^{-2}$. A generalized vector dominance model, GVDM [71], which has an additional piece varying as $(1 + Q^2/m_0^2)^{-1}$, was also examined. A very naive model adds the VDM and QPM contributions to account for low- and high-Q^2 regions. The GVDM already contains a point-like piece to simulate the QPM portion, but it is still possible to imagine adding the GVDM and QPM contributions.

The TPC/2γ data are shown in Figure 11.1 for four regions of the $\gamma\gamma$ c.m. energy, W. The combination GVDM + QPM does not describe the data since it does not fall fast enough with increasing Q^2. The pure VDM describes the data at high W well, but falls too rapidly with increasing Q^2 for low W. Both the GVDM and VDM+QPM describe the data reasonably well except in the lowest W region.

The cross section for $\gamma\gamma$ at $Q^2 = 0$ has also been extracted from the TPC/2γ data (using GVDM). The results are compared with earlier results from PLUTO [72] and the 2γ Collaboration [73] in Figure 11.2. The rise in the cross section in the PLUTO data at low W is not confirmed. In fact, subsequent data from the PLUTO Collaboration itself failed to confirm their earliest results [74].

The AMY Collaboration at TRISTAN has reported on the structure function, F_2, measured at an average value of Q^2 of 67 GeV^2, based on about 40 events [70]. In Fig. 11.2 the data are shown, together with fits based on QPM + VDM, for three values of the cutoff introduced by Field, Kapusta, and Poggioli. It is clear that the data that exist are adequately represented by this form. More data are needed to distinguish definitively between the various models considered in this Figure.

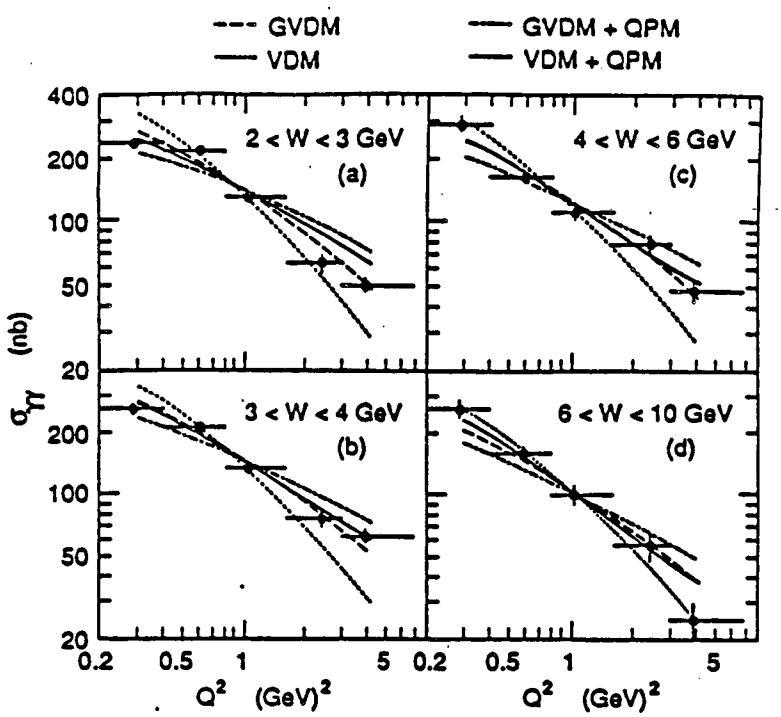

Figure 11.1: Data from the TPC/2γ Collaboration for the $\gamma\gamma$ total cross section compared to simple theoretical models.

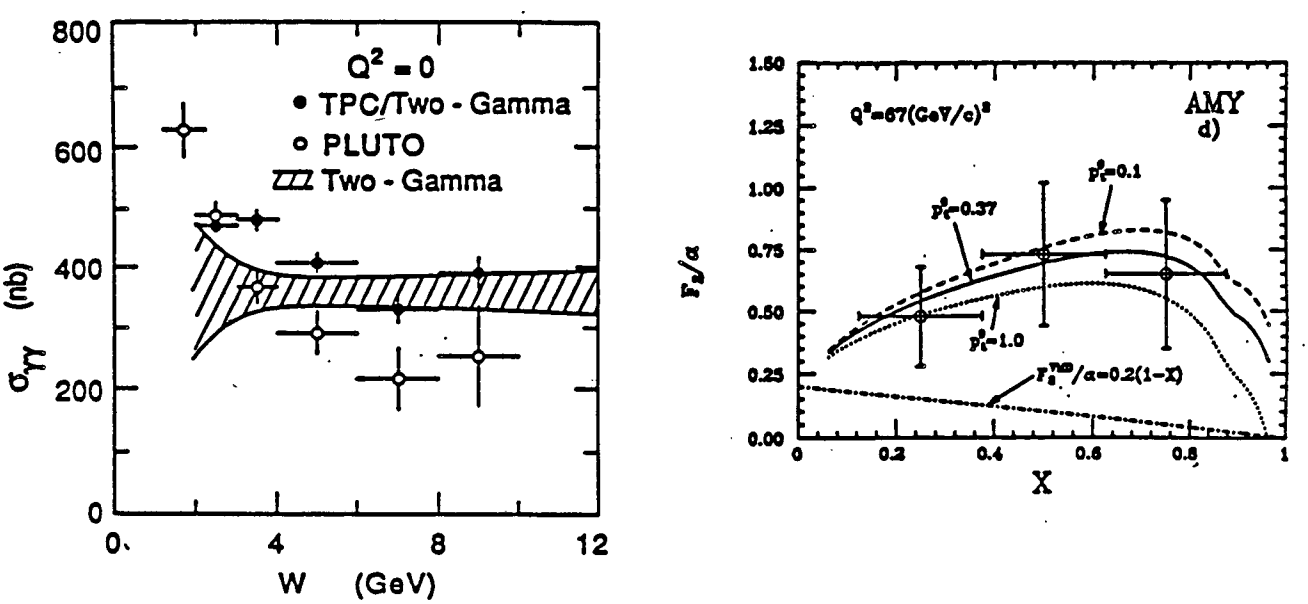

Figure 11.2: Results on the $\gamma\gamma$ cross section at high and low Q^2. On the left, data from the TPC/2γ Collaboration [69] at $Q^2 = 0$ compared with results from PLUTO [72] and the 2γ Collaboration [73]. On the right, data from the AMY Collaboration [70] at an average value of $Q^2 = 67$ GeV^2 compared to fits with QPM + VDM for various values of the p_t cutoff.

12 Prospects for High-Energy $\gamma\gamma$ Collisions

The beginning of LEP and the prospect of LEP II might suggest that we are entering a era of high-energy $\gamma\gamma$ collisions. Unfortunately this is not so. The Low formula for production of a resonance of spin J may be written

$$\sigma(e^+e^- \to e^+e^-R) = \eta^2 \frac{(2J+1)8\pi^2\Gamma(R\to\gamma\gamma)}{m_R^3} \times \left[\left(2+\frac{m_R^2}{s}\right)\ln\frac{s}{m_R^2} - 2\left(1-\frac{m_R^2}{s}\right)\left(3+\frac{m_R^2}{s}\right)\right] \tag{12.1}$$

where nominally

$$\eta = (\alpha/2\pi)(\ln s/m_e^2). \tag{12.2}$$

Actually η reflects the available phase space and is cutoff by form factors at a scale nearer m_R^2 than s. Altogether, at fixed m_R, $\sigma(e^+e^- \to e^+e^-R)$ grows approximately as $\ln s/m_e^2$ as s increases. Of course the event rates depend on the luminosity, $\mathcal{L}$, as well as a σ. The luminosities and energies of some e^+e^- machines are shown in Table 12.1. In Fig. 12.1 we show the number of events that would be produced at four machines with an integrated luminosity of 100 pb^{-1} for a $J=0$ resonance with $\Gamma(R\to\gamma\gamma) =$ 1 keV. Since resonances like η_c have small branching ratios into reconstructable channels, at least 100 or more events are needed. Increasing the energy from that of CESR to that of LEP expands the range of resonances accessible from about 3 GeV to about 6 GeV. To explore a higher mass range a completely different technique is required.

Machine	Energy	L (cm^{-2}s^{-1})
PEP	15 + 15	$7\cdot10^{31} - 3\cdot10^{32}$
PETRA	22 + 22	†
DORIS	5 + 5	$4\cdot10^{31}$
CESR	5 + 5	$10^{32} - 5\cdot10^{32}$
TRISTAN	30 + 30	$2\cdot10^{31}$
LEP	50 + 50	$6\cdot10^{30} - 1\cdot10^{32}$

Table 12.1: Luminosities and energies of selected e^+e^- machines. PETRA is no longer operating.

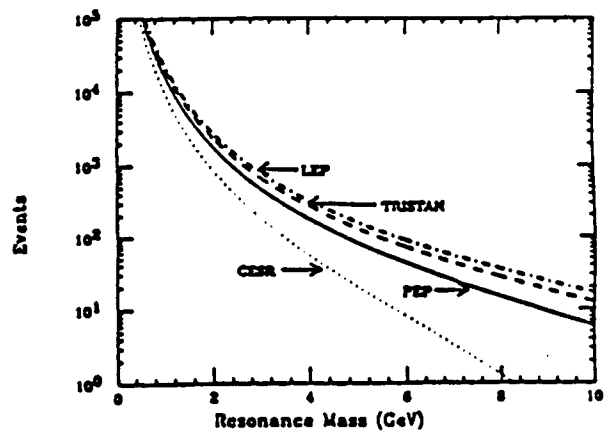

Figure 12.1: The number of events that would be produced with an integrated luminosity of 10^{38} cm^{-2} for a $J=0$ resonance with $\Gamma(R\to\gamma\gamma) = 1$ keV at four machines.

13 Beamstrahlung

In linear e^+e^- colliders electrons (or positrons) in one bunch are deflected by the field of the other bunch. As a result, the electrons emit synchrotron radiation. Himel and Siegrist [75] estimated the effect by relating it to deflection by a magnetic field whose strength would give the same radius of curvature of the path as in the bunch – bunch collision. They used known results, including quantum corrections, for the deflection in a magnetic field. The problem was taken up by Blankenbecler and Drell [76,77] who did a thorough quantum mechanical calculation, finding results in substantial agreement with Himel and Siegrist. The problem has also been addressed by Jacob and Wu [78,79] and by Bell and Bell [81].

In fact, the general problem of quantum corrections to synchrotron radiation was solved much earlier by Baier and Katkov [82,83]. They showed that the quantum mechanically correct results may be obtained from the classical results by a simple modification of the energy variable, as described below.

To understand the classical result we consider the frame in which one bunch is at rest. The incident particles have momentum $P = m\Gamma = 2m\gamma^2$ in this frame (and momentum $m\gamma$ in the beam-beam cms). The stationary cylindrical bunch has length L, radius B, and uniform charge density. Inside the bunch the electrostatic field is radial with strength

$$|eE| = \frac{2\alpha N}{BL}\frac{b}{B}, \tag{13.1}$$

where N is the number of electrons or positrons in the bunch. The radius of curvature, ρ, of the path of the incident particle is determined by

$$a = \frac{v^2}{\rho} = \frac{eE}{m\Gamma}, \tag{13.2}$$

and the arc subtends an angle

$$\frac{L}{\rho} = \frac{2\alpha N}{mB\Gamma} \equiv \frac{2y}{\Gamma}\frac{b}{B}, \tag{13.3}$$

from the center of curvature, where y is a parameter introduced by Blankenbecler and Drell [76]. A

	SLC	TLC	Super
N	$5 \cdot 10^{10}$	10^{10}	$3 \cdot 10^8$
E	50 GeV	325 GeV	5 TeV
B	10^{-4} cm	$7 \cdot 10^{-6}$ cm	$5 \cdot 10^{-8}$ cm
l_0	10^{-1} cm	$6 \cdot 10^{-2}$ cm	$3 \cdot 10^{-5}$ cm
y	140	400	2000
C	50	1.5	10^{-5}
δ_0	0.014	1.3	$2 \cdot 10^8$

Table 13.1: Parameters for the SLC and two hypothetical e^+e^- colliders [76,77].

second parameter, C, is defined by

$$C = \frac{m^2}{\Gamma(eE)_{max}} = \frac{m^2BL}{2N\alpha\Gamma}. \tag{13.4}$$

Values of these and other parameters for three machines are shown in Table 13.1.

The critical frequency for synchrotron radiation is [84]

$$\omega_c = \frac{3\Gamma^3}{\rho}, \tag{13.5}$$

in terms of which the classical synchrotron radiation spectrum is [84]

$$\frac{dI}{d\omega} = 2\sqrt{3}\alpha\Gamma\frac{\omega}{\omega_c}\int_{2\omega/\omega_c}^{\infty} dx\, K_{5/3}(x). \tag{13.6}$$

To apply this to our problem, two changes are required. First, the result must be multiplied by $(\pi y/2\Gamma)(b/B)$, the fraction the arc makes of a full circle. Second, we must use Eq. (13.6) only up to the maximum energy, ω_q, that the electron could possibly emit:

$$\omega_q = m\Gamma = \frac{CB}{3b}\omega_c. \tag{13.7}$$

If we introduce the dimensionless variable $x = \omega/\omega_q$ and calculate the photon number spectrum, averaging over impact parameter, we find

$$\frac{dN}{dx} = \frac{2\alpha yC}{\sqrt{3}\pi}\xi^2\int_{\xi}^{\infty}\left(\frac{1}{\xi^2} - \frac{1}{z^2}\right)K_{5/3}(z)dz, \tag{13.8}$$

where

$$\xi = 2Cx/3. \tag{13.9}$$

Now the full result of Blankenbecler and Drell for spinless particles [76] is

$$\frac{dN}{dx} = \frac{2\alpha y(1-x)}{x} u^{1/2} \int_u^\infty \left(\frac{3}{2}v - u - \frac{u^4}{2v}\right) Ai(v)dv, \tag{13.10}$$

where Ai is the Airy function and

$$u^3 = [Cx/(1-x)]^2. \tag{13.11}$$

Judicious integrations by parts and use of recursion relations show that this may be written

$$\frac{dN}{dx} = \frac{2\alpha y C}{\sqrt{3}\pi} \xi'^2 \int_{\xi'}^\infty \left(\frac{1}{\xi'^2} - \frac{1}{z^2}\right) K_{5/3}(z)dz. \tag{13.12}$$

where

$$\xi' = \frac{2Cx}{3(1-x)} \tag{13.13}$$

This is in perfect accord with the result of Baier and Katkov, who show that for dN/dx the quantum mechanical result is obtained by replacing x with $x/(1-x)$ [82,83].

For a Dirac particle the result is simply Eq. 13.12 multiplied by $1 + \frac{1}{2}x^2/(1-x)$.

14 Heavy Ions

Heavy ions have been considered recently as a potential source for high-energy $\gamma\gamma$ collisions, possibly using the LHC or SSC. The advantage of heavy ions is that the cross section varies as $Z^4\alpha^4$ rather than just as α^4. Of course there is a cost: the process must be coherent, that is, the nucleus must survive intact.

A straightforward calculation of the flux, including the nuclear form factor, gives [85]

$$\frac{dN}{dx} = \frac{Z^2\alpha}{\pi x} \int_{x^2M^2}^\infty \frac{dQ^2}{Q^2} F(Q^2)^2 \left(1 - \frac{x^2M^2}{Q^2}\right). \tag{14.1}$$

If the source were instead an electron, the form factor would be absent as would the x^2M^2/Q^2 term. Setting the upper limit of integration to s would give $dN/dx \approx (\alpha/\pi x)\ln(s/m_e^2)$, in agreement with the usual Weizsäcker-Williams form

$$\left[\frac{dN}{dx}\right]_{WW} = \left(\frac{\alpha}{\pi x}\ln\frac{s}{4m_e^2}\right)\frac{1}{2}[1+(1-x)^2]. \tag{14.2}$$

Drees et al. approximated

$$F(Q^2)^2 = \exp(-Q^2/Q_0^2), \tag{14.3}$$

with $Q_0 = 55 - 60$ MeV for Pb. For $x << 1$ this gives

$$\left[\frac{dN}{dx}\right]_{DEZ} = \frac{Z^2\alpha}{\pi x}\left(\ln\frac{Q_0^2}{(xM)^2} - 1.577\right). \tag{14.4}$$

In an earlier work Papageorgiu used [86]

$$\left[\frac{dN}{dx}\right]_P = \frac{Z^2\alpha}{\pi x}\ln\frac{1}{(xMR)^2}, \tag{14.5}$$

where R is the nuclear radius, $R \approx 1.2A^{1/3}$f, $1/R \approx 165A^{1/3}$ MeV. To compare these approximations we write

$$\left[\frac{dN}{dx}\right]_{DEZ} = \frac{Z^2\alpha}{\pi x}\left(\ln\frac{1}{(xMR)^2} - 1.577 + \ln Q_0^2R^2\right) \tag{14.6}$$

For Pb, $\ln Q_0^2R^2 = 1.40$, so the DEZ result is just slightly smaller than that of Papageorgiu.

If the nucleus were never disrupted by the collision it would still be necessary to include the electromagnetic form factor. However, here we want to study a rather delicate process, $\gamma\gamma \to X$, in an environment dominated by Pb Pb$\to$ *horrible mess*. This requires that we consider only events in which the nuclei do not physically collide.

Indeed, as regards the nuclei, the process is classical. The equivalent photon approximation should be calculated in impact parameter space, restricting the events to those with impact parameter $b > 2R$. The result is [87]

$$\left[\frac{dN}{dx}\right]_d = \frac{2Z^2\alpha}{\pi x}\left\{\left(\frac{x}{x_0}\right)K_0\left(\frac{x}{x_0}\right)K_1\left(\frac{x}{x_0}\right) - \frac{1}{2}\left(\frac{x}{x_0}\right)^2\left[K_1^2\left(\frac{x}{x_0}\right) - K_0^2\left(\frac{x}{x_0}\right)\right]\right\}. \tag{14.7}$$

where

$$x_0 = \frac{1}{b_{min}M}. \tag{14.8}$$

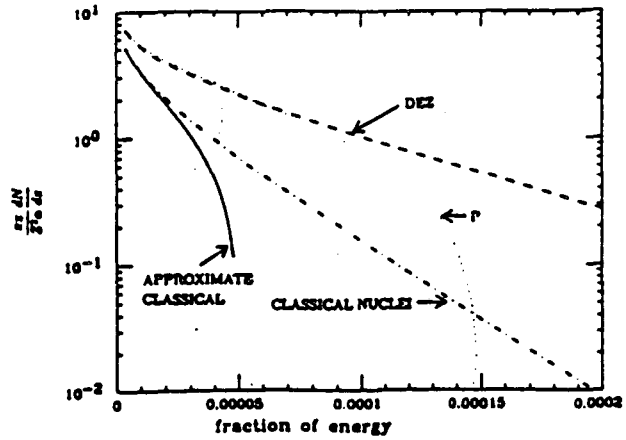

Figure 14.1: Various approximations to the equivalent photon flux from a heavy ion beam. The quantity $(\pi x/Z^2\alpha)(dN/dx)$ is shown as a function of x, the fraction of the ion's momentum given to the photon. The result of Drees et al. [85], Eq. (14.1), is shown as the dashed curve. The result of Papageorgiu, [86], Eq. (14.5), is shown as a dotted curve. The full classical result, Eq. (14.7), is shown as a dot-dashed curve. The low-momentum approximation to the full classical result, Eq. (14.9), is shown as a solid curve.

For very small values of x this becomes

$$\left[\frac{dN}{dx}\right] = \frac{Z^2\alpha}{\pi x}\left[\ln\frac{1}{(xMR)^2} - 2.15\right], \qquad (14.9)$$

a result that is substantially below those of Drees et al. and Papageorgiu. Moreover, as seen in Fig. 14.1, this difference becomes greater as x increases.

15 Linacs and Backscattering

High-energy photon beams have regularly been obtained by scattering laser light from linac beams. Recently H. Sens has promoted this as a technique for $\gamma\gamma$ scattering [88]. The potential is impressive.

For a 3 eV photon colliding with a 50 GeV electron beam, the c.m. energy of the Compton scattering is $\sqrt{s} = \sqrt{m_e^2 + 4E_eE_\gamma} = 0.86$ GeV. With a sufficiently intense laser beam, every electron gets scattered by a photon, so the photon flux is essentially equal to that of the initial electron flux. The

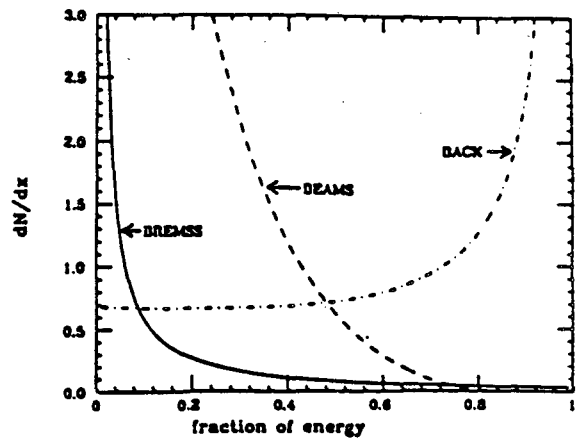

Figure 15.1: Equivalent photon spectra that could be obtained from an electron beam with energy 325 GeV. The solid curve shows the Weizsäcker-Williams spectrum, Eq.(14.2). The beamstrahlung spectrum, the dashed curve, is shown for $C = 1.5, y = 400$ [76,77]. The spectrum from the backscattered laser beam, Eq. (15.1), is shown as the dot-dashed curve for the same electron energy and photon energy $k = 2$ eV.

energy distribution of the photons is determined by the differential cross section for Compton scattering boosted to the appropriate frame. It is easy to show that

$$\frac{dN}{dx} = \frac{1 - x + \frac{1}{1-x} - \frac{4x}{y(1-x)} + \frac{4x^2}{y^2(1-x)^2}}{(1-4/y+8/y^2)\ln(1+y)+1/2+8/y-(1+y)^{-2}/2} \qquad (15.1)$$

where

$$x = k'/E, \quad y = 4Ek/m_e^2, \qquad (15.2)$$

and E (E') is the incident (final) electron energy and k (k') is the incident (final) photon energy. The collision is assumed to be head-on. This spectrum is compared to that from beamstrahlung and the usual Weizsäcker-Williams spectrum in Fig. 15.1.

16 WW Collisions

The Lepton-Photon Conference is by now the Electroweak Conference, and so it makes sense to consider the electroweak variants of $\gamma\gamma$ scattering: WW and ZZ scattering. In 1983 it was realized that this

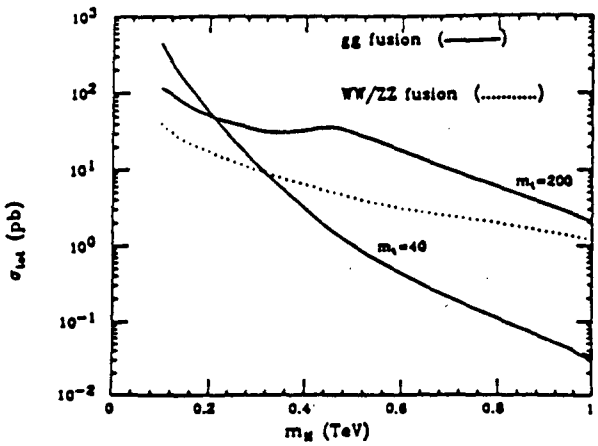

Figure 16.1: The Higgs boson production cross section in pp collisions at $\sqrt{s}$ = 40 TeV as a function of the Higgs boson mass. The dotted curve shows the contribution from WW and ZZ fusion. The solid curves are for gluon-gluon fusion for two values of the t quark mass. Ref. [93]

process would dominate the production of an orthodox Higgs boson at the SSC if the mass of the Higgs boson were about 300 GeV or more [89]. Shortly thereafter the equivalent flux of Ws and Zs from a high-momentum quark was calculated [90,91,92], with the result for the longitudinal and transverse bosons

$$\begin{aligned} \frac{dN_L}{dx} &= \frac{g_V^2+g_A^2}{8\pi^2 x}\ln\frac{s}{m_W^2}[1+(1-x)^2] \\ \frac{dN_T}{dx} &= \frac{g_V^2+g_A^2}{8\pi^2 x}2(1-x). \end{aligned} \tag{16.1}$$

Here, for WW collisions, $g_V = -g_A = e/(\sin\theta_W 2\sqrt{2})$. It is the longitudinal Ws and Zs that dominate [89]. In the equivalent W approximation $\sigma(ud \to duH)$ via the WW intermediate state is given by [90],

$$\sigma = \frac{1}{16m_W^2}\left(\frac{\alpha}{\sin^2\theta_W}\right)^3[(1+\tau)\ln(1/\tau)-2+2\tau], \tag{16.2}$$

where $\tau = m_H^2/s$. This competes with another $\gamma\gamma$ analogue, gluon-gluon fusion. The cross section for Higgs boson production in pp scattering at $\sqrt{s} = 40$ TeV is shown in Fig. 16.1.

17 Higgs Boson Production

The best hope for the discovery of a very massive Higgs boson, with $m_H > 200$ GeV, is a very high energy hadron collider like the SSC. The decay $H \to ZZ$ followed by decays of the Z into electrons or muons provides the best signature. However, if the Higgs boson has a mass less than twice the mass of the Z, the task is complicated [94]. If the mass is greater than about 125 GeV it is possible to look for the decay into one real Z and one virtual Z in the charged leptonic channels. Finding a 100 GeV Higgs boson would certainly be difficult at the SSC, since its primary decay would be to $b\bar{b}$, for which the QCD-generated background would be stupendous. This provides motivation for considering the production of a 100 GeV Higgs boson at an electron-positron collider.

The same WW fusion mechanism, $e^+e^- \to \nu\bar{\nu}W^+W^- \to \nu\bar{\nu}H$ would be available at an e^+e^- collider [95]. Using Eq. (16.2), for $\sqrt{s} = 2E_{beam} = 1$ TeV, the cross section is about $3\cdot 10^{-37}\text{cm}^2$. Despite the absence of a purely hadronic background, there remain some serious problems, especially if the mass of the Higgs boson is near that of the W. A very substantial integrated luminosity is required, perhaps 30 fb^{-1}.

An alternative is $\gamma\gamma$ collisions. The observed cross section is related to the $\gamma\gamma$ luminosity relative to the e^+e^- luminosity,

$$\mathcal{L}_{rel} = \mathcal{L}_{\gamma\gamma}/\mathcal{L}_{e^+e^-}, \tag{17.1}$$

by

$$\sigma_{Higgs\ via\ \gamma\gamma} = \left[\frac{8\pi^2}{m_H^3}\Gamma(H\to\gamma\gamma)\right]\tau\frac{d\mathcal{L}_{rel}}{d\tau} \tag{17.2}$$

Since the $\gamma\gamma$ width of a 100 GeV Higgs boson is a few keV, the factor in square brackets is a few times 30 fb. Since $\tau\frac{d\mathcal{L}_{rel}}{d\tau}$ is of order 1, the resulting cross section is roughly equivalent to that of $e^+e^- \to \nu\bar{\nu}W^+W^- \to \nu\bar{\nu}H$. Fig. 15.1 shows that both beamstrahlung and backscattering produce photon fluxes that are substantial for mo-

menta that are a good fraction of the beam energy. With electron-positron luminosities in the range $10^{34}\,\mathrm{cm}^{-2}\,\mathrm{s}^{-1}$ these techniques could be capable of producing a large number of 100 GeV Higgs bosons.

Drees et al. estimated that lead-lead collisions in the SSC with a luminosity of a few times $10^{26}\,\mathrm{cm}^{-2}\,\mathrm{s}^{-1}$ would be adequate for the purpose. This value may need to be revised upward in view of the reductions displayed in Fig. 14.1.

18 Summary and Prospects

Two-photon physics continues to challenge us both theoretically and experimentally. While the pseudoscalar and tensor multiplets are quite well understood, there are significant puzzles among the scalars and axial vectors. New, high statistics experiments could provide results that would resolve important ambiguities. With the increasing reliability of lattice calculations of the QCD spectrum, there will be more and more interest in understanding both the $q\bar{q}$ and non-$q\bar{q}$ mesons, and two-photon physics can provide unique insights into these particles.

Understanding the dynamics of nonresonant hadronic final states is especially difficult. A profusion of data on the vector-vector final state has demonstrated once again how hard this is. The brave application of perturbative QCD to exclusive final states has achieved mixed results, but these may improve in time. Although the data for the structure function of the photon continue to grow, the time of precision measurements has not yet arrived.

In the short term, the frontier in two-photon physics is the frontier of integrated luminosity. The differences between the energies of the various operating e^+e^- machines have only a small significance. Only accumulated events count. The outstanding work done by many of the collaborations on the $f_1(1425)$ testifies to the potential for two-photon physics. While there may be more immediate interest in B or Z physics, there is work of lasting value to be done with $\gamma\gamma$ collisions.

In the long term, the high-energy frontier can be extended in $\gamma\gamma$ collisions only by the introduction of novel accelerator techniques: beamstrahlung, backscattered laser beams, and heavy ions. It is too soon to know how practical these will prove to be, but it is not too soon to start thinking about them.

References

[1] J. Olsson, *Proc. XIII International Symposium on Lepton and Photon Interactions, Nucl. Phys.* B (Proc. Suppl.) 3, 613 (1988).

[2] H. Kolanoski and P. Zerwas, "Two-Photon Physics" in *High Energy Electron-Positron Physics*, Eds. A. Ali and P. Söding, World Scientific, 1988.

[3] S. Cooper, *Ann. Rev. Nucl. Part. Sci.* 38, 705 (1988).

[4] *Proceedings of the VIIIth International Workshop on Photon-Photon Collision*, Shoresh, Israel, April 24 - 28, 1988. Ed. U. Karshon World Scientific, 1988.

[5] F. Low, *Phys. Rev.* **120**, 582 (1960).

[6] N. A. Roe et al, "Measurement of the Two-photon Width of the η and η'," SLAC-PUB 4931, accepted for publication in *Phys. Rev.* D.

[7] F. Butler, "Resonant Production in Two Photon Collisions," LBL-26465. The results here must be corrected by a factor ≈ 1.15, see J. H. Boyer in [17].

[8] J. K. Bienlein, "Observed and Unobserved States - Crystal Ball Results on Two-Photon Physics," in *Glueballs, Hybrids, and Exotic Hadrons*, A. I. P. Conference Proceedings No. 185, Ed. S.-U. Chung, p. 486.

[9] See, for example, F. J. Gilman and R. Kauffman, *Phys. Rev.* **D36**, 2761 (1987).

[10] J. F. Donoghue, B. R. Holstein, and Y-C. R. Lin, *Phys. Rev. Lett.* **55**, 2766 (1985).

[11] J. Gasser and H. Leutwyler, *Nucl. Phys.* **B250**, 465 (1985).

[12] S. J. Brodsky and G. P. Lepage, *Phys. Rev.* **D24**, 1808 (1981).

[13] TPC/2γ Collaboration , "Investigation of the Electromagnetic Structure of η and η' Mesons by Two-Photon Interactions, submitted to this conference.

[14] Crystal Ball Collaboration, H. Marsiske, *Proceedings of the VIII th International Workshop on Photon-Photon Collisions*, Shoresh, Israel, April 24 -28, 1988, Ed. U. Karshon, p. 15.

[15] JADE Collaboration, J. Olsson, *Proceedings of the VIII th International Workshop on Photon-Photon Collisions*, Shoresh, Israel, April 24 -28, 1988, Ed. U. Karshon, p. 77.

[16] CELLO Collaboration, J. Harjes, *Proceedings of the VIII th International Workshop on Photon-Photon Collisions*, Shoresh, Israel, April 24 -28, 1988, Ed. U. Karshon, p. 85.

[17] Mark II Collaboration, J. Boyer, *Proceedings of the VIII th International Workshop on Photon-Photon Collisions*, Shoresh, Israel, April 24 - 28, 1988, Ed. U. Karshon, p. 94; J. H. Boyer, "Two Photon Production of Pion Pairs in e^+e^- Collisions at 29 GeV," LBL-27180.

[18] TOPAZ Collaboration, I. Adachi et al., submitted to this conf[illegible]ence.

[19] PLUTO Collaboration, M. Feindt, *Proceedings of the VIII th International Workshop on Photon-Photon Collisions*, Shoresh, Israel, April 24 -28, 1988, Ed. U. Karshon, p. 3.

[20] Crystal Ball Collaboration, D. Antreasyan et al., *Phys. Rev.* **33**, 1847 (1986).

[21] Crystal Ball Collaboration, B. Muryn, *Proceedings of the VIII th International Workshop on Photon-Photon Collisions*, Shoresh, Israel, April 24 -28, 1988, Ed. U. Karshon, p. 102.

[22] CELLO Collaboration, H. -J. Behrend et al., submitted to this conference.

[23] H. J. Lipkin, *Proceedings of the VIII th International Workshop on Photon-Photon Collisions*, Shoresh, Israel, April 24 -28, 1988, Ed. U. Karshon, p. 107.

[24] TASSO Collaboration, W. Braunschweig et al., *Z. Phys.* **41**, 533 (1989).

[25] TPC/2γ Collaboration, H. Aihara et al., *Phys. Rev. Lett.* **60**, 2355 (1988).

[26] G. Gidal et al., Proceedings of the XXII International conference on High Energy Physics, Berkeley, CA (1986), World Scientific, Vol. II, p. 1220

[27] CLEO Collaboration, T. Jensen et al., reported at Cornell Meeting on Heavy Quark Physics, June, 1989.

[28] C. Baglin et al., *Phys. Lett.* **187B**, 191 (1987).

[29] M. S. Chanowitz, "Resonances in Photon-Photon Scattering," *Proceedings of the VIII th International Workshop on Photon-Photon Collisions*, Shoresh, Israel, April 24 -28, 1988, Ed. U. Karshon, p. 205.

[30] R. L. Jaffe, *Phys. Rev.* **D15**, 267 (1977); R. L. Jaffe and K. Johnson, *Phys. Lett.* **60B**, 201 (1976).

[31] J. Weinstein and N. Isgur, [illegible]*ys. Rev. Lett.* **48**, 659 (1982); *Phys. Rev.* **D2**[illegible] 588 (1983).

[32] R. L. Goble, R. Rosenfeld [illegible]nd J. L. Rosner, *Phys. Rev.* **D39**, 3264 (1[illegible]) and references therein.

[33] J. F. Donoghue, B. R. Holstein, and Y. C. Lin, *Phys. Rev.* **D37**, 2423 (1987).

[34] J. Bijnens and F. Cornet, *Nucl. Phys.* **B296**, 557 (1988).

[35] M. R. Pennington, *Proceedings of the VIII th International Workshop on Photon-Photon Collisions*, Shoresh, Israel, April 24 -28, 1988, Ed. U. Karshon, p. 297.

[36] M. S. Chanowitz, Proc. VI International Workshop of Photon-Photon Interactions, Ed. R. Lander, World Scientific, 1984, p.95.

[37] M. Feindt,"1988 CELLO, JADE, and PLUTO - Contributions to 'Exotic' Meson Spectroscopy," in *Glueballs, Hybrids, and Exotic Hadrons*, A. I. P. Conference Proceedings No. 185, Ed. S.-U. Chung, p. 501.

[38] TPC/2γ Collaboration, H. Aihara et al., *Phys. Rev. Lett.* **57**, 51 (1986).

[39] M. Feindt, "Experimentelle Untersuchung der Reaktionen $\gamma\gamma \to K_S^0 K^{\pm}\pi^{\mp}$ und $\gamma\gamma \to K_S^0 K_S^0$ mit dem Detektor PLUTO," DESY F14-88-02.

[40] PLUTO Collaboration, Ch. Berger et al., *Z. Phys.* **37**, 329 (1988).

[41] CELLO Collaboration, H.-J. Behrend et al., *Z. Phys.* **42**, 367 (1989).

[42] CELLO Collaboration, H.-J. Behrend et al., *Z. Phys.* **43**, 91 (1989).

[43] Mark II Collaboration, G. Gidal et al., *Phys. Rev. Lett.* **59**, 2016 (1987).

[44] F. M. Renard, *Nuovo Cimento* **80A**, 1 (1984).

[45] R. N. Cahn, "Twos in Two-Photon Physics," *Proceedings of the VIII th International Workshop on Photon-Photon Collisions*, Shoresh, Israel, April 24 -28, 1988, Ed. U. Karshon, p.110.

[46] M. S. Chanowitz, *Phys. Lett.* **B187**, 409 (1987).

[47] R. N. Cahn, *Phys. Rev.* **D35**, 3342 (1987).

[48] See the reviews by G. Gidal "Radiative Widths of Resonances (Experiments)," in *Proceedings of the VIII th International Workshop on Photon-Photon Collisions*, Shoresh, Israel, April 24 -28, 1988, Ed. U. Karshon, p. 182, and "Resonance Formation in Photon-Photon Collisions," in *Glueballs, Hybrids, and Exotic Hadrons*, A. I. P. Conference Proceedings No. 185, Ed. S.-U. Chung, p. 171.

[49] W. Bartel et al., *Phys. Lett.* **184B**, 288 (1987); A. J. Finch, "Inclusive D^* Production in Single Tagged $\gamma\gamma$ Events," in *Proceedings of the VIII th International Workshop on Photon-Photon Collisions*, Shoresh, Israel, April 24 -28, 1988, Ed. U. Karshon, p. 75.

[50] TPC/2γ Collaboration, F. C. Erné, "Exclusive and Inclusive Charm Production in Photon-Photon Collisions," in *Proceedings of the VIII th International Workshop on Photon-Photon Collisions*, Shoresh, Israel, April 24 -28, 1988, Ed. U. Karshon, p. 71.

[51] TASSO Collaboration, W. Braunschweig et al., "Study of Charmed Meson Production in $\gamma\gamma$ Interactions," submitted to this conference.

[52] G. Alexander, U. Maor, and P. G. Williams, *Phys. Rev.* **D26**, 1198 (1982); G. Alexander, A. Levy, and U. Maor, *Z. Phys.* **C30**, 65 (1986).

[53] N. N. Achasov, S. A Deryanin, and G. N. Shestakov, *Phys. Lett.* **B108**, 134 (1982); *Z. Phys.* **C16**, 55 (1982); ibid. **C27**, 99 (1985).

[54] B. A. Li and K. F. Liu, *Phys. Lett.* **B118**, 435 (1982); ibid. **B124**, 55 (1982); *Phys. Rev. Lett.* **51**, 1510 (1983); *Phys. Rev.* **D30**, 613 (1984).

[55] S. J. Brodsky, G. Köpp, and P. M. Zerwas, *Phys. Rev. Lett.* **58**, 443 (1987).

[56] A. W. Nilsson, "Exclusive Final States - Continuum (Experimental)" in *Proceedings of the*

VIII th International Workshop on Photon-Photon Collisions, Shoresh, Israel, April 24 -28, 1988, Ed. U. Karshon, p. 261.

[57] U. Maor, "Vector Meson Production in $\gamma\gamma$ Reactions," in *Proceedings of the VIII th International Workshop on Photon-Photon Collisions*, Shoresh, Israel, April 24 -28, 1988, Ed. U. Karshon, p. 282.

[58] N. N. Achason and G. N. Shestakov, *Phys. Lett.* **203B**, 309 (1988).

[59] B. A. Li and K.-F. Liu, "$K^*\overline{K}^*$ Mesonium Production in $\gamma\gamma$ Reactions and Hadronic Collisions," University of Kentucky preprint, UK/89-02, submitted to this conference.

[60] ARGUS Collaboration, "Two-Photon Production of Final States with a $p\bar{p}$ Pair," DESY 88-194.

[61] TPC/2γ Collaboration, H. Aihara et al., "Exclusive Production of $p\bar{p}\pi^+\pi^-$ in Photon Photon Collisions," NIKHEF-H/89-9.

[62] G. R. Farrar, E. Maina, and F. Neri, *Nucl. Phys.* **B259**, 702 (1985).

[63] G. R. Farrar, et al., "Perturbative QCD Predictions for $\gamma\gamma \rightarrow B\overline{B}$, *Proceedings of the VIII th International Workshop on Photon-Photon Collisions*, Shoresh, Israel, April 24 -28, 1988, Ed. U. Karshon, p. 43.

[64] E. Witten, *Nucl. Phys.* **B120**, 189 (1977).

[65] Ch. Berger and W. Wagner, *Phys. Rep. C* **146**, 1 (1987).

[66] J. H. Field, F. Kapusta, and L. Poggioli, *Phys. Lett.* **181B**, 362 (1986); J. H. Field "Structure Functions and Total Cross Sections," in *Proceedings of the VIII th International Workshop on Photon-Photon Collisions*, Shoresh, Israel, April 24 -28, 1988, Ed. U. Karshon, p. 349.

[67] W. Frazer, *Phys. Lett.* **B194**, 287 (1987).

[68] W. Frazer and G. Rossi, *Phys. Rev.* **D25**, 843 (1982).

[69] TPC/2γ Collaboration, H. Aihara et al., "A Measurement of the Total Hadronic Cross Section in Tagged $\gamma\gamma$ Reactions," submitted to this conference.

[70] AMY Collaboration, "A Measurement of the Photon Structure Function F_2 at an Average Q^2 of 67 $(\mathrm{GeV}/c)^2$," submitted to this conference.

[71] J. J. Sakurai and D. Schildknecht, *Phys. Lett.* **40B**, 121 (1972).

[72] Ch. Berger et al., *Phys. Lett.* **149B**, 421 (1984).

[73] D. Bintinger et al., *Phys. Rev. Lett.* **54**, 763 (1985).

[74] M. Feindt, "Recent PLUTO Results on Photon Photon Reactions," in *VIIth International Workshop on Photon-Photon Collisions,* Ed. A. Courau and P. Kessler, World Scientific, 1986, p. 388.

[75] T. Himel and J. Siegrist, "Quantum Effects in Linear Collider Scaling Laws," SLAC-PUB-3572, 2nd International Workshop on Laser Acceleration of Particles, Los Angeles, Jan. 7-18, 1985.

[76] R. Blankenbecler and S. D. Drell, *Phys. Rev.* **D36**, 277 (1987).

[77] R. Blankenbecler and S. D. Drell, *Phys. Rev. Lett.* **61**, 2324 (1988), Erratum *ibid.* **62**, 116 (1989).

[78] M. Jacob and T. T. Wu, *Phys. Lett.* **197B**, 253 (1987).

[79] M. Jacob and T. T. Wu, *Nucl. Phys.* **B303**, 373 (1988).

[80] M. Jacob and T. T. Wu, *Nucl. Phys.* **B303**, 389 (1988).

[81] M. Bell and J. S. Bell, CERN-TH 5174/88.

[82] V. N. Baier and V. M. Katkov, *Phys. Lett.* **25A**, 492 (1967).

[83] V. N. Baier and V. M. Katkov, *Sov. Phys. JETP* **26**, 854 (1968).

[84] J. D. Jackson, *Classical Electrodynamics*, 2nd Edition, Wiley, 1975, p.677.

[85] M. Dress, J. Ellis, and D. Zeppenfeld, *Phys. Lett.* **B223**, 454 (1989).

[86] E. Papageorgiu, *Phys. Rev.* **D40**, 92 (1989).

[87] J. D. Jackson, *Classical Electrodynamics*, 1st Edition, Wiley, 1962, p. 523.

[88] H. Sens, "Critical Issues and Prospects for Future Work," in *Proceedings of the VIII th International Workshop on Photon-Photon Collisions*, Shoresh, Israel, April 24 -28, 1988, Ed. U. Karshon, p.143.

[89] R. N. Cahn and S. Dawson, *Phys. Lett.* **136B**, 196 (1984).

[90] M. S. Chanowitz and M. K. Gaillard, *Phys. Lett.* **142B**, 85 (1984); *Nucl. Phys.* **B261**, 379 (1985).

[91] S. Dawson, *Nucl. Phys.* **B249**, 42 (1985).

[92] G. L. Kane, W. W. Repko, and W. B. Rollnick, *Phys. Lett.* **148B**, 367 (1984).

[93] J. F. Gunion, G. L. Kane, and J. Wudka, *Nucl. Phys.* **299**, 231 (1987).

[94] See, for example, R. N. Cahn, *Rep. Prog. Phys.* **52**, 389 (1989).

[95] See, for example, C. Ahn et al., "Opportunities and Requirements for experimentation at High Energy e^+e^- Collider," SLAC-329, 1988.

LAWRENCE BERKELEY LABORATORY
UNIVERSITY OF CALIFORNIA
INFORMATION RESOURCES DEPARTMENT
1 CYCLOTRON ROAD
BERKELEY, CALIFORNIA 94720